Martin-Biosca, Y.; Escuder-Gilabert, L.; Medina-Hernandez, MJ.; Sagrado Vives, S. (2018). Modelling the enantioresolution capability of cellulose tris(3,5-dichlorophenylcarbamate) stationary phase in reversed phase conditions for neutral and basic chiral compounds. Journal of Chromatography A. 1567:111-118. https://doi.org/10.1016/j.chroma.2018.06.061

Title: Modelling the enantioresolution capability of cellulose tris(3,5-dichlorophenylcarbamate) stationary phase in reversed phase conditions for neutral and basic chiral compounds

Authors: Yolanda Martín-Biosca, Laura Escuder-Gilabert, María José Medina-Hernández, Salvador Sagrado

PII: S0021-9673(18)30817-3
DOI: https://doi.org/10.1016/j.chroma.2018.06.061
Reference: CHROMA 359505

To appear in: *Journal of Chromatography A*

Received date: 14-3-2018
Revised date: 31-5-2018
Accepted date: 25-6-2018

Please cite this article as: Martín-Biosca Y, Escuder-Gilabert L, Medina-Hernández MJ, Sagrado S, Modelling the enantioresolution capability of cellulose tris(3,5-dichlorophenylcarbamate) stationary phase in reversed phase conditions for neutral and basic chiral compounds, *Journal of Chromatography A* (2018), https://doi.org/10.1016/j.chroma.2018.06.061

Modelling the enantioresolution capability of cellulose tris(3,5-dichlorophenylcarbamate) stationary phase in reversed phase conditions for neutral and basic chiral compounds

Yolanda Martín-Biosca[1], Laura Escuder-Gilabert[1*], María José Medina-Hernández[1*], Salvador Sagrado[1,2]

[1]Departamento de Química Analítica, Universitat de València, Burjassot, Valencia, Spain

[2] Instituto Interuniversitario de Investigación de Reconocimiento Molecular y Desarrollo Tecnológico (IDM), Universitat Politècnica de València, Universitat de València, Valencia, Spain

Corresponding authors at: Departamento de Química Analítica, Facultat de Farmacia, Universitat de València, Avda. Vicent Andrés Estellés, s/n, E-46100 Burjassot, Valencia, Spain.
E-mail addresses: maria.j.medina@uv.es (Ph. D. M.J. Medina); lescuder@uv.es (Ph. D. L. Escuder)

Highlights

~~Immobilised cellulose tris(3,5-dichlorophenylcarbamate) modelled as chiral stationary phase in reversed phase conditions.~~

Rs model for immobilised cellulose tris(3,5-dichlorophenylcarbamate) in chiral RPLC

~~Experimental enantioresolution of structurally unrelated drugs and pesticides connected to their topological and molecular descriptors.~~

Enantioresolution-topological/molecular descriptor model for unrelated compounds

~~The pH-dependent molar total charge of the molecule as key variable for enantioresolution.~~

The pH-dependent molar total charge as key variable for enantioresolution.

Parameter related to the chiral carbon connected with enantioresolution

Protocol for enantioseparation anticipation

ABSTRACT

To the best of our knowledge, the prediction of the enantioresolution ability of polysaccharides-based stationary phases in liquid chromatography for structurally unrelated compounds has not been previously reported. In this study, structural information of neutral and basic compounds is used to model their enantioresolution levels obtained from an immobilised cellulose tris(3,5-dichlorophenylcarbamate) stationary phase in reversed phase conditions. Thirty-four structurally unrelated chiral drugs and pesticides, from seven families, are studied. Categorical enantioresolution levels (*RsC*, 0 = no baseline enantioresolution and 1 = baseline enantioresolution) are established from the experimental enantioresolution values obtained at a fixed experimental conditions. From 58 initial structural variables, three topological parameters (two of them connected to the chiral carbon), and six molecular descriptors (one of them also related with the chiral carbon), are selected after a discriminant partial least squares refinement process. The molar total charge of the molecule at the working pH is the most important variable. The relationships between *RsC* and the most important structural variables and the drug/pesticide family are evaluated. An explicit model is proposed to anticipate the *RsC* levels, which provides 100% of correct anticipations. A criterion is introduced to alert about the compounds that should not be anticipated.

Keywords:
Cellulose tris(3,5-dichlorophenylcarbamate) stationary phase
Reversed phase liquid chromatography
Enantioseparations
Enantioresolution modelling
Discriminant partial least squares

1. Introduction

Chiral molecules play an important role in life and medicinal sciences as well as in other fields such as food and environmental chemistry. Consequently, analytical techniques capable of differentiating between enantiomers are of great importance. Chromatographic and capillary electromigration techniques are the most employed analytical separation techniques [1-5].

Due to its simplicity and accuracy, high-performance liquid chromatography (HPLC) with chiral stationary phases (CSPs) is one of the most widely used analytical technique for enantiomeric separations. The basis of analytical enantioseparations, in the so-called direct approach, is the formation of transient diastereomeric complexes between the compound and the chiral selector coated or immobilized onto the stationary phase. Different CSPs containing macromolecular selectors (i.e. proteins, polysaccharide derivatives, polymers, etc.), macrocyclic selectors (i.e. cyclodextrins, macrocyclic antibiotics, etc.) and low-molecular mass selectors (i.e. ligand exchange, chiral ion exchange, etc.) have been developed [1]. More than a hundred CSPs are offered commercially and about 20–30 CSPs are the most frequently employed [4].

In spite of the wide number of analytical applications of CSPs in HPLC, the fundamental mechanisms responsible for the observed chiral separations are not fully understood. In fact, today, the evaluation of the ability of a chiral column in HPLC for the enantioseparation of compounds is an expensive and time-consuming trial-and-error strategy. Thus, the prediction of whether a CPS is able to perform a chiral separation or not is of great benefit. Relatively few articles in the literature address this important issue in chiral HPLC method development.

Polysaccharide based stationary phases represent by far the most widely used CSPs in HPLC due to their broad applicability for a large structural diversity of compounds. These CSPs, which can be coated or immobilised onto the stationary support, are cellulose- and amylose-based. These linear helical polymers are composed of glucose units with β (1→4) (cellulose) or α(1→4) (amylose) linkages. The hydroxyl groups of the glucose molecules are derivatised with benzoate or phenylcarbamate moieties, which accept methyl groups and/or chlorine substituents in various positions

on the aromatic ring, yielding a large variety of derivatives with different selectivities and applications [2-5]. Even, differences in enantioseparations between the CPSs containing the same chiral selector either coated or covalently immobilised onto the surface of silica have been achieved [4].

Selector-selectand complexes are thought to be mediated via hydrogen bonds to the CO or NH groups of the carbamate moieties, as well as by π- π interactions between the phenyl rings, Van der Waals forces and steric factors [3, 5-8]. Recently, halogen bonding has been also described to contribute to selector-selectand complexation [9].

In chiral HPLC using polysaccharides-based stationary phases, normal, polar or reversed mobile phase conditions can be used. The mobile phase composition modulates the recognition process. Different chromatographic behaviours are obtained depending on the nature and composition of the mobile phase, due to changes produced in the intra-molecular hydrogen bonds of the polysaccharide structure. Thus, reversal of the elution order enantiomers depending on the composition of the mobile phase can be observed [4].

In order to elucidate the chiral recognition mechanism of polysaccharide chiral selectors, analytical separation techniques in combination with spectroscopic techniques such as NMR spectroscopy, Fourier transform and attenuated total reflectance IR spectroscopy, vibrational circular dichroism techniques as well as X-ray crystallography have been used [1-8]. Molecular modelling has also become a practical tool for evaluating the interactions between polysaccharide-based selectors and chiral compounds [2, 10].

Chemometric and chemoinformatic data mining methods might be helpful to extract valuable information on molecular recognition [11-12]. Among these,

quantitative structure–property relationships (QSPRs) are a powerful option. Different QSPR studies have been reported for modelling data in enantioselective chromatography using polysaccharides-based stationary phases, some of them are presented/reviewed in the paper by Del Rio [11]. In these QSPR models, enantioresolution-related information (retention or selectivity values) is correlated with different molecular properties of compounds through linear free energy relationships (LFERs) studies [13-16], linear solvation energy relationships (LSERs) [17], and 3D-QSPR properties employing comparative molecular field analysis (CoMFA) [18]. Multiple linear regression (MLR) [15-17], artificial neural networks [18], and genetic algorithm [16, 18] are used as chemometric techniques.

These studies are usually carried out for structurally related compounds using amylose and cellulose-based CSPs -amylose tris(3,5-dimethylphenylcarbamate) [13, 15], cellulose tris(3,5-dimethylphenylcarbamate) [18] and immobilised amylose tris(5-chloro-2-methylphenylcarbamate) [16]-, and normal and polar mobile phases. In these studies, information about the functional groups responsible for enantioresolution is usually obtained. It should be noted that resolution values between enantiomers have never been used as response variable, although it is the most practical term that describes how well two peaks are resolved.

In previous papers [19-20], the enantioresolution level (*RsC*-level) of structurally unrelated basic drugs and pesticides, using sulfated β- and γ-cyclodextrins as chiral selectors in electrokinetic chromatography (EKC), was modelled as a function of structural parameters. For sulfated β-cyclodextrin, few structural descriptors, easy to obtain from a free on-line database, were selected [19]. In the case of sulfated γ-

cyclodextrin, few topological parameters, mainly connected to the chiral carbon (so called *C**-parameters) were used [20].

In this work, 58 structural predictor variables of 34 structurally unrelated compounds (basic drugs and pesticides), previously assayed in the above-mentioned papers, are tested to model a categorical enantioresolution *RsC*, as response variable. The main aim is to define a protocol able to anticipate the enantioresolution (*RsC* = 1) or not (*RsC* = 0) of new compounds based on this model. The *RsC* levels are assigned from experimental enantioresolution (*Rs*) values obtained using an immobilised cellulose tris(3,5-dichlorophenylcarbamate) CSP and hydro-organic mobile phases. To the best of our knowledge, this is the first report that models the enantioresolution of structurally unrelated compounds separated using immobilised cellulose tris(3,5-dichlorophenylcarbamate) CSP and hydro-organic mobile phases. On the other hand, the importance of the predictive power (*Pp*) statistic to assess a discriminant partial least squares for one response categorical variable (DPLS1) refinement is discussed. In addition, the relationships between *RsC* and the most important structural variables and the drug/pesticide family are evaluated.

2. Materials and methods

2.1. Instrumentation

An Agilent Technologies 1100 chromatograph (Palo Alto, CA, USA) with a binary pump, an UV–visible diode array detector, a column thermostat and an autosampler was used. Data acquisition and processing were performed by means of the LC/MSD ChemStation software (B.04.02 SP1 [208], ©Agilent Technologies 2001-2010).

Prior to injection into the chromatographic system, analytes solutions were filtered through disposable 0.22 μm polyethersulphone syringe filters (Frisenette, Knebel, Denmark). Mobile phase solutions were vacuum-filtered through 0.22 μm Nylon membranes (Micron Separations, Westboro, MA, USA) and were degassed in an Elmasonic S60 ultrasonic bath (Elma, Singen, Germany) prior to use. A Crison MicropH 2000 pHmeter (Crison Instruments, Barcelona, Spain) was employed to adjust the pH of the buffer solutions.

2.2. Chemicals and solutions

All reagents were of analytical grade. Ammonium acetate, sodium dihydrogen phosphate monohydrate, sodium hydroxide, acetonitrile and methanol (®Multisolvent, HPLC grade) were from Scharlau, S.L. (Barcelona, Spain). Diethylamine was from Acros Organics (Geel, Belgium). 10 mM ammonium acetate buffer solution was prepared by dissolving the appropriate amount of ammonium acetate in water and adjusting the pH to 8.0 with 2.5 M sodium hydroxide. Ultra Clear TWF UV deionised water (SG Water, Barsbüttel, Germany) was used to prepare solutions.

Bicalutamide, brompheniramine maleate, carbinoxamine maleate, chlorpheniramine maleate, clemastine fumarate, doxylamine succinate, ethopropazine hydrochloride, fenfluramine, hydroxyzine hydrochloride, methadone hydrochloride, methotrimeprazine maleate, nomifensine maleate, orphenadrine hydrochloride, pindolol, terfenadine, trimeprazine hemi(+)-tartrate and verapamil hydrochloride were from Sigma (St. Louis, MO, USA). Citalopram hydrobromide was from Tokyo Chemical Industry (Tokyo, Japan). Promethazine hydrochloride and salbutamol sulfate were from Guinama (Valencia, Spain). Bupivacaine was from Caiman Chemical Co (Ann Arbor, MI, USA). Amlodipine was from Alfa Aesar (Karlsruhe, Germany). All the rest of drugs tested were kindly donated by several pharmaceutical laboratories: acebutolol hydrochloride by Italfarmaco (Madrid, Spain); atenolol by Zeneca Farma (Madrid, Spain); fluoxetine hydrochloride by Alter (Madrid, Spain); mepivacaine hydrochloride and prilocaine hydrochloride by Laboratorios Inibsa (Barcelona, Spain); metoprolol tartrate by Ciba Geigy (Barcelona, Spain); propanocaine by Laboratorio Seid (Barcelona, Spain); propranolol hydrochloride by ICI Farma (Madrid, Spain); timolol maleate by Merck Sharp & Dohme (Madrid, Spain); and viloxazine hydrochloride by Astra Zeneca (Cheshire, UK). All racemic pesticides (benalaxyl, hexaconazole, imazalil, myclobutanil, metalaxyl and penconazole) were from Dr. Ehrenstofer (Augsburg, Germany).

Stock standard solutions of compounds used in this study were prepared by dissolving 10 mg of the racemic mixture in 10 mL of methanol. Working solutions were prepared by dilution of the stock standard solutions using the mobile phase solution. The solutions were stored under refrigeration at 5°C.

2.3. Methodology for the chiral separation of compounds

The experimental enantioresolution (*Rs*) values of the compounds listed in Table 1 were obtained using an immobilised cellulose tris(3,5-dichlorophenylcarbamate) column (Chiralart Cellulose-SC; 3 μm, 150 × 4.6 mm i.d.; YMC Separation Technology Co., Ltd.; Tokyo, Japan). A ternary mixture consisting of ammonium acetate buffer (10 mM, pH 8) / acetonitrile / diethylamine (60/40/0.1, v/v/v) was used as mobile phase. The mobile phase flow rate was 1.0 mL min^{-1} and the injection volume was 2 μL. The detection was performed in the UV at 220 nm for all compounds, except for ethopropazine, methotrimeprazine, promethazine and trimeprazine whose detection was performed at 254 nm. The column was thermostatted at 25 °C.

2.4. Software and calculations

Most of the structural variables used in this study were taken from the online ChemSpider chemical structure database [21] and were previously assayed in a study to anticipate the experimental enantioresolution of chiral compounds in electrokinetic chromatography using two sulfated cyclodextrins as chiral selectors [19, 20]. The first seven variables ($\mathbf{x_1}$ to $\mathbf{x_7}$) correspond to the C^*-parameters. These parameters are calculated as the count of atoms/groups bonded to the chiral carbon (C^*), for instance C^*X (C^*-heteroatoms) and C^*hA (C^*-aromatic heterocycles) [20]. Variables $\mathbf{x_8}$ to $\mathbf{x_{25}}$ correspond to molecular descriptors predicted by ACD/Labs and ChemAxon calculations: minimal z length (*zmin*), molecular surface area (*MSA*), orbital electronegativity of the chiral carbon atom (*OEC**) and surface tension (*ST*), among others. Variables $\mathbf{x_{26}}$ to $\mathbf{x_{55}}$ correspond to molecular topological parameters predicted by ChemAxon; for instance, aromatic ring count (*Arc*). In addition, from the molecular

descriptor logarithm of octanol–water partition coefficient (log*P*, from ACD/Labs), variable $\mathbf{x_{56}}$, two additional variables ($\mathbf{x_{57}}$ and $\mathbf{x_{58}}$), the apparent log*P* at a given pH (log*D*) and the molar total charge (α), were calculated in this work at pH 8 (the working pH), using the following equations [22]:

$$\log \delta_i = \log\left(\frac{\beta_i h^i}{1 + \beta_1 h + \beta_2 h^2 + \cdots + \beta_i h^i + \cdots + \beta_n h^n}\right) \quad (1)$$

$$\log D = \log P + \log \delta_i \quad (2)$$

$$\alpha = \sum_{j=0}^{n} a_j \delta_j \quad (3)$$

In these equations, δ_i is the molar fraction of the neutral form of the compound, h is the proton concentration (i.e. $h = 10^{-8}$ M at pH 8.0), β_i is the protonation cumulative constant (for a polyprotic system, $\beta_n = K_1 \cdot K_2 \cdot \ldots \cdot K_i \cdot \ldots \cdot K_n$), a_j is the value with its sign of the net charge of the considered specie (i.e. -1, 0, +1, +2, …) and δ_j the molar fraction of the considered specie at the considered pH. The values of the logarithm of the protonation constants (log*K*) used to calculate the molar fractions were taken from the literature [23].

It should be noted that log*D* is available from ACD/Labs only at pH 5.5 and 7.4, so we preferred to use eqs. 1 and 2 to perform the calculation at the experimental pH (8) used to obtain the enantioresolution data. On the other hand, α (eqs. 1 and 3), non-included in the above-mentioned papers [19, 20], was introduced for the first time in this work as a potential predictor variable for enantioresolution.

Principal component analysis (PCA) and ~~discriminant partial least squares, for one response categorical variable (~~DPLS1~~)~~ models have been performed using The Unscrambler® v.9.2 multivariate analysis software [24].

During DPLS1 model refinement (variable selection stage), the predictive power, *Pp*, has been used as the optimization parameter to define the effective predictive ability of the model. *Pp* was calculated using the following equation [25]:

$$Pp = 2EV_{CV} - EV \quad (4)$$

where *EV* is the explained variance and EV_{CV} its cross-validated value for the response variable. A value of $Pp \geq 55\%$ has been considered acceptable for discriminant models [19].

3. Results and discussion

3.1. Experimental and categorised enantioresolution

Table 1 shows the experimental enantioresolution data (*Rs*) obtained using the screening procedure depicted in section 2.3 for the compounds studied (Table S1 in supplementary data includes the 2D structure of the compounds). Compounds are arranged according to their drug/pesticide families. In previous papers dealing with enantioresolution modelling in EKC, the modelling of categorised (*RsC*) instead of experimental *Rs* values were recommended [19, 20]. The use of a categorical *RsC* variable to be modelled and predicted fits the main aim of the present paper, which is just to anticipate whether a new compound will be enantioresolved or not in the chromatographic conditions assayed. So, the experimental *Rs* values were converted into categorised *RsC* values (see Table 1). Compounds showing baseline

enantioresolution (e.g. *Rs* ≳ 1.7; *No* = 1, 5, 6, 7, 8, 9, 23 and 24 in Table 1) were assigned to *RsC* = 1. The rest of compounds were assigned to *RsC* = 0, with the exception of propranolol (*No* 27; *Rs* = 1.4), for which an *RsC* = 0.5 was selected, taking into account that it is close to the baseline enantioresolution in these conditions.

3.2. Structural influence (influential compounds)

The detection and elimination of influential compounds with dissimilar structure is of utmost importance prior to developing any kind of model. These compounds could disturb the internal structure of latent variables of the further DPLS1 model, so they should be eliminated to avoid the alteration of structure-enantioresolution relationships. In order to detect possible influential compounds, a PCA analysis was performed ~~(see details in supplementary data).~~ For this purpose, the structural information described in section 2.4 were organised into a 34×58 **X**-matrix. The options autoscaled data and leave-one-out (LOO) cross-validation were chosen.

Figure 1A shows the PC1-PC2 bi-plot showing the scores (relationships between compounds) and loadings (relationships between variables). As can be observed, terfenadine and verapamil (*No* 22 and 33, respectively, in Table 1; whose scores are indicated in the plot) have differential scores in the direction of a superimposed axis (dashed line). This axis represents a large set of correlated variables related to the molecular size (e.g. variables $\mathbf{x}_{18}$, *MSA* and $\mathbf{x}_{23}$, *MM*). For instance, the molecular mass (*MM*) of the compounds *No* 22 and 33 are 471.70 and 454.60 Da, respectively. However, the rest of compound have *MM* values in the 238.33 to 336.43 Da range. The molecular surface area (*MSA*; from Chem Axon) is another example of molecular dissimilarity. Whereas *MSA* values of the compounds 22 and 33 are 780.90 and 797.90

Å^2, respectively, for the rest of compound are in the 374.70 to 579.98 Å^2 range. Thus, fixing threshold limits for one or two of these variables could enable to identify new influential compounds without the need to perform a new PCA analysis.

Figure 1B shows the Influence plot (Residual vs. Leverage) for compounds. It confirms that terfenadine and verapamil are influential (high leverage), in agreement with the results obtained in previous papers [19, 20]. Influential compounds (with different structures from the majority) could disturb the structure-*RsC* relationship and should be eliminated.

3.3. Modelling the structure-RsC relationship (DPLS1) and variable selection process

DPLS1 modelling was selected to relate the structural data (**X**-matrix) to the *RsC* data (**y**-vector), as suggested in previous papers [19, 20]. To build the DPLS1 model, the influential compounds *No* 22 and 33 were omitted. As in the PCA analysis, autoscaled data and the LOO cross-validation options were used.

Several criteria were adopted to optimise the model. Ideally, the model should fit the following goals: (i) A primary goal is to achieve full discrimination between the group of compounds with predicted *RsC* = 0 and 1, for the calibration outputs (all compounds in the model), and if possible, for the cross-validated outputs; (ii) The predictive power *Pp* has to be ≥ 55%, (the recommended level [19]); (iii) The optimal number of latent variables (k_o) has to be close to 1, for instance, k_o = 1 or 2 (k_o = 1, is the ideal value here since there is just one response variable, *RsC*); (iv) The final model has to have significant or almost significant variables (i.e. **b** ± **Ub** does not include zero).

The initial DPLS1 model derived provided full discrimination between compounds having *RsC* = 0 and 1 in the calibration set (see Fig. S1 in supplementary data). Therefore, this initial model fits the primary goal of this work. However, some compounds were misclassified in the cross-validated outputs (mainly *No* 1 and 23, validation plot in Fig. S1). In addition, other negative aspects were also observed. A poor predictive power was obtained, *Pp* = 0, due to an excessive distance between *EV* and $EV_{CV,}$ 78.3% and 30.6%, respectively. This fact also justifies the differences in the prediction success rates between the calibration and cross-validated outputs. On the other hand, a value of k_o = 4 was obtained (far from the ideal one), indicating an excessive model complexity. Finally, the scaled regression coefficients indicate that practically all the variables were non-significant, with the exception of $\mathbf{x_4}$ (*C*hA)*, $\mathbf{x_{57}}$ (log*D)* and $\mathbf{x_{58}}$ (α). These three variables will probably remain in the final model, but most of the rest would contribute negatively to the poor predictive ability of the current model.

Model refinement (e.g. elimination of noisy variables, that is, those with the worst **Ub/b** ratios) has proven to be convenient in order to improve its performance. Also *Pp* has been proposed to control the progress of refinement instead of other more common parameters as *EV* or EV_{CV} [19 and references therein]. In the present study, the process of model refinement was performed in two stages, due to the high number of variables. In addition, the *Pp* value was used as an indicator to control the quality of the model.

In the first refinement stage, the elimination of noisy variables was carried out in turn in several steps, deleting up to 4 variables at each step. The process was stopped when the remaining variables in the model showed comparable importance (comparable

b ± **Ub** values). In this case, model refinement was stopped for 15 remaining variables. Figure 2 shows the evolution of the parameters k_o and *EV*, EV_{CV} and *Pp* while decreasing the number of variables into the model during this refinement stage. As can be expected, the values of *Pp* raise and k_o decrease along the process, indicating an improvement in the quality of the model.

On the other hand, as can be seen in Figure 2, the use of *EV* (related with the calibration set) to control the refinement progress is not adequate in this case. The model refinement from 35 to 31 remaining variables resulted in a decrease in the *EV values*, due to the change from $k_o = 4$ to $k_o = 2$. This decrease in the *EV* values suggests an apparent loss of predictive ability that would lead to incorrectly stopping the refinement process. EV_{CV} seems to be a better diagnostic indicator. However, from 31 to 24 remaining variables (with $k_o = 2$), there is a stabilization of the parameter (even a little decrease) that would incorrectly suggest no further improvement, as in the case of *EV*. Therefore, *Pp* (relating both calibration and cross-validated outputs) is the best option to measure the improvement of the DPLS1 model. *Pp* also exhibits a higher relative slope (improvement) than EV_{CV}. To the best of our knowledge, this is the first time that the superiority of *Pp* to control model refinement, compared with other more conventional criteria, is outlined. In fact, a high *Pp* value guaranties a short distance between calibration and cross-validated predictions (i.e. the model robustness) and, as a consequence, can assure the achievement of the primary goal mentioned above.

In the second refinement stage, the elimination of variables was performed one by one, eliminating each time that one whose elimination greatly improved *Pp*, without affecting negatively the others consolidated rules. This stage was stopped when the elimination of any new variable worsen the quality of the model (*Pp* or any other

feature). Some technical details of the final model can be seen in supplementary data (Fig S2). Only nine variables, with acceptable **b** ± **Ub** values, remained in the final model: two chiral-topological parameters, $\mathbf{x_1}$ and $\mathbf{x_4}$ (C^*X and C^*hA, respectively), a molecular topological parameter, $\mathbf{x_{36}}$ (*Arc*) and six molecular descriptors, $\mathbf{x_{11}}$, $\mathbf{x_{18}}$ $\mathbf{x_{21}}$, $\mathbf{x_{25}}$, $\mathbf{x_{57}}$ and $\mathbf{x_{58}}$ (*zmin*, *MSA*, *OEC**, *ST*, log*D* and α, respectively).

The model exhibited good discrimination between predicted *RsC* = 0 and 1 data for calibration, and cross-validated outputs. It exhibited, a *Pp* value of 56% (*EV* = 78.4% and EV_{CV} = 67.4%), with k_o = 2, near to the ideal value. So, the model was considered satisfactory for the purpose of this work. The values of the variables included in the final model for the compounds studied are shown in Table 2.

3.4. RsC-variables relationships

The magnitude of the scaled regression coefficients (**b**-magnitude) reflects the importance of each selected variable to describe the enantioresolution. Positive **b**-values indicate positive contributions (i.e. a high value of the variable favours the enantioresolution) and vice versa. According to this, α (negative contribution) is the variable that contributes the most to enantioresolution since its coefficient doubles the importance over the other variables (see Fig S2 in supplementary data). Therefore, neutral and low charged compounds (α close to zero) have a priori the largest probability of enantioresolution.

The other eight variables of the model have similar importance between them (similar coefficient magnitudes). This fact indicates that their contribution to the enantioresolution is almost equivalent. The absence of heteroatoms or aromatic heterocycles (C^*X and C^*hA; negative coefficients) directly linked to the chiral carbon

(*C**), as well as the presence of the aromatic rings in the molecule (aromatic ring count (*Arc*); positive contribution), also improve the enantioresolution. In the same way, low *zmin* and *MSA* values and high *OEC**, *ST* and log*D* values enhance the enantioresolution. It should be noted that log*D* but not log*P* was selected to obtain the final model. Thus, for ionisable compounds, the effective hydrophobicity, adjusted with the mobile phase pH, could contribute to improve the enantioresolution.

As stated in the introduction section, the results obtained confirm that hydrophobic, electronic and steric factors are the main interactions responsible of enantiorecognition in polysaccharide-based stationary phases.

As can be seen in Table 2, seven of the enantioresolved compounds (*No* = 5, 6, 7, 8, 9, 23 and 24) have low α values (in the 0 – 0.33 range), while the majority of the non-enantioresolved compounds have $\alpha > 0.92$. This behaviour is in agreement with that previously stated. However, for some compounds the contribution of the rest of variables becomes more important than the effect of α. For example, although nomifensine (*No* 1) has a relatively high α value (0.88; unfavourable for *RsC*), it is enantioresolved due to the combination of other favourable parameters (e.g. it has the lowest *MSA* value, 374.7 $Å^2$). On the contrary, enantioresolution was not achieved for metalaxyl (*No* 10) despite being a neutral compound ($\alpha = 0$; favourable for *RsC*). This molecule has, for instance, one *C*X* (the C*-N bound) and just one aromatic ring (*Arc* = 1), among other non-favourable contributions (see Table 2).

Figure 3 shows the final DPLS1 score plot. Scores are labelled by their ordered numbers (*No* in Table 1; Figure 3A), *RsC* values (Figure 3B~~, upper part~~) and their families (Figure 3C~~, lower part~~). As can be seen, compounds having *RsC* = 1 are located in the right space, which is logical attending the *RsC* position in the loading plot (Fig.

S2 in supplementary data). These points correspond to the family 2 (fungicides, except metalaxyl, *No* 10) and to two local anaesthetics and one antidepressant (families 4 and 1, respectively). In the central part of the score plot, several families are mixed, all of them with *RsC* = 0. β-blockers (family 5, *RsC* = 0) are located in the left upper quadrant, except propranolol (*No* 27), the only compound close to the baseline enantioresolution (*RsC* = 0.5). Thus, the DPLS1 results are discreetly conditioned by the families of the compounds studied.

3.5. Explicit model for enantioresolution anticipation

In order to easily anticipate whether or not a new compound will be enantioresolved, a practical explicit model was derived from DPLS1. For this purpose, raw (de-scaled) coefficients were calculated from the scaled ones. The following equation was obtained (eq. 5):

$$eRs = -1.28 - 0.14\ C^{*}X - 0.22\ C^{*}hA - 0.078\ zmin - 0.0022\ MSA + 0.25\ OEC^{*} + 0.024\ ST + 0.22\ Arc + 0.072\ \log D - 0.57\ \alpha \quad (5)$$

where *eRs* refers to an output related to *Rs* that should be seen as an indicative value since categorical *Rs* data were used to obtain the model. Figure 4 shows the *eRs* outputs obtained from eq. 5 *vs* the initial assigned *RsC* values (Table 1) for the compounds of the calibration set.

To anticipate enantioresolution, *eRs* outputs have to be transformed into anticipated-*RsC* (*aRsC*) outputs, comparable to the categorical (*RsC*) levels previously stablished. For this purpose, as Figure 4 shows, it is necessary to apply the following rules: (i) *aRsC* = 1, full enantioresolution, for *eRs* > 0.5; (ii) *aRsC* = 0.5, almost full

enantioresolution, for *eRs* between 0.4 and 0.5 and (iii) *aRsC* = 0, poor or no enantioresolution, for *eRs* < 0.4.

Alternatively, a simpler approach can be applied to establish if a molecule will be completely enantioresolved (*aRsC* = 1) or not (*aRsC* = 0). In this case, *aRsC* levels (0 or 1) are calculated by directly rounding the *eRs* values to integer numbers (without decimal digits). Table 2 shows the *aRsC* values obtained by applying this direct rule. Such anticipations are identical to those obtained by applying the previous rules, except for propranolol (*RsC* = 0.5) as expected. For this compound, this approach anticipates no full enantioresolution (*aRsC* = 0), which strictly agrees with the experimental result, *Rs* = 1.4. An anticipation success rate of 100% was obtained by comparing *aRsC* (Table 2) and *RsC* assignations from experimental data (Table 1).

3.6. Protocol for a safe aRsC anticipation and additional remarks

A complete protocol to perform a safe *aRsC* anticipation for a new compound in the current conditions is:

- Step-1a. Obtain *MSA* from ChemAxon (this value will be necessary in further steps). Optionally, obtain the molecular mass (*MM*).
- Step-1b. If *MSA* is outside the 350 – 600 $Å^2$ range the anticipation is not recommended (for more security, anticipation should not be done if *MM* is outside the 200 - 350 Da range). Otherwise, continue to the next steps.
- Step-2a. Locate the chiral carbon (*C**) in the 2D structure of the chiral compound. Find the presence or absence of *C**-heteroatoms (*C***X*) and *C**-aromatic heterocycles (*C***hA*) bonds. Assign a value to these parameters according to the

criteria: *C*X* presence (1); *C*X* absence (0); *C*hA* presence (1); *C*hA* absence (0). Count the aromatic rings in the whole molecule (*Arc* is also provided by ChemAxon).

- Step-2b. Use ChemAxon to calculate the values of the variables *zmin*, *MSA*, *OEC**, *ST* and p*Ka*. From ACD/LogP estimate log*P*.
- Step-2c. Calculate log*D* and α at pH 8, according to eqs. 1-3.
- Step-3. Use eq. 5 to estimate *eRs*. Round this value to an integer number for a rapid anticipation of enantioresolution, (a*RsC* only 0 or 1). Alternatively, use the following criteria for a 3-level *aRsC*: baseline enantioresolution (*aRsC* = 1) if *eRs* > 0.5, poor or non enantioresolution (*aRsC* = 0) if *eRs* < 0.4, and almost full enantioresolution (*aRsC* = 0.5) if *eRs* is in the 0.4 – 0.5 range.

The LOO cross-validation strategy performed on the final DPLS1 model is virtually equivalent to the use of an external validation strategy [25]. Note that in this approach, the prediction, in turn, of each single compound (acting at that moment as an external validation sample), is made with a model very close to the final model (just excluding the compound to be predicted).

On the other hand, to test the anticipative ability of the protocol with compounds non included to build the model, four molecules (fenfluramine, amlodipine, bupivacaine and bicalutamide), satisfying the step-1b of the protocol, were first anticipated and then chromatographed for experimental confirmation. Table 3 shows the values of the predictive variables, the anticipated output (*aRsC*; consistent with Step 3 of the protocol) and the corresponding experimental *Rs* values. In all cases, experimental enantioresolution values confirmed the anticipation.

The compounds included in this study are structurally unrelated (drugs and pesticides) compounds. Except fungicides (compounds *No* 5-10), which are neutral, all are basic compounds, most of them fully ionised at pH = 8.0. *A priori*, the anticipation protocol should be applicable for compounds of similar nature, in experimental conditions similar to those used in this study (section 2.3).

4. Conclusions

Structural information of structurally unrelated chiral compounds can be connected with experimental enantioresolution data in HPLC obtained using immobilised cellulose tris(3,5-dichlorophenylcarbamate) column in reversed phase conditions. Safe anticipation of the categorised (i.e. favourable/unfavourable) enantioresolution is possible. It requires a precise discriminant PLS-based (DPLS1) multivariate study; i.e. combining scaled regression coefficients and their uncertainty intervals with the predictive power (*Pp*) values for a consistent model refinement. Such study provides double valuable information: (i) the variables more informative and their contribution (positive or negative) to the enantioresolution of a compound (descriptive function), and (ii) an explicit equation to anticipate its enantioresolution (predictive function).

From 58 initial structural variables, three topological parameters (two of them connected to the chiral carbon), and six molecular descriptors (one of them also related with the chiral carbon), are selected after a discriminant partial least squares refinement process. The topology surrounding the chiral carbon is a relevant aspect on enantioresolution. However, in this case, the molar total charge, which depends on the mobile phase pH (α), becomes the most important descriptor. Accordingly, the

enantioresolution of neutral or low charged basic compounds is favoured. On the other hand, the model discriminates between two of the families studied, fungicides and β-blockers.

A stepwise protocol facilitates the anticipation of the enantioresolution without the need of the previous derived models. It includes threshold limits, based on the topological parameter aromatic ring count, to detect influential compounds whose anticipation becomes risky. Applying the protocol, an anticipation success rate of 100% for the compounds studied is obtained, when compared with the experimental results. The high *Rs*-anticipation effectiveness found suggests that the strategy could serve for other RPLC or in general HPLC chiral methods.

Finally, for a given chiral selector, the experimental enantioresolution values depend on the chiral stationary phase features (batch, immobilisation chemistry, supplier, etc.). This is the main reason why a categorical instead of quantitative *Rs* variable is used in this work. It is expected that the qualitative output (*aRsC* = 0 or 1) proposed could be transferred to other columns, although it should be confirmed with experimental results.

Acknowledgements: The authors acknowledge the Spanish Ministerio de Economía y Competitividad (MINECO) and the European Regional Development Fund (ERDF) for the financial support (Project CTQ2015-70904-R, MINECO/FEDER, UE).

The authors declare no conflict of interest.

References

[1] M. Lämmerhofer, Chiral recognition by enantioselective liquid chromatography: Mechanisms and modern chiral stationary phases, J. Chromatogr. A 1217 (2010) 814–856.

[2] G.K.E. Scriba, Chiral recognition mechanisms in analytical separation sciences, Chromatographia 75 (2012) 815-838.

[3] G.K.E. Scriba, Chiral recognition in separation science-an update, J. Chromatogr. A 1467 (2016) 56–78.

[4] B. Chankvetadze, Recent developments on polysaccharide-based chiral stationary phases for liquid-phase separation of enantiomers, J. Chromatogr. A 1269 (2012) 26–51.

[5] J. Shen, Y. Okamoto, Efficient separation of enantiomers using stereoregular chiral polymers, Chem. Rev. 116 (2016) 1094–1138.

[6] Y. Okamoto, T. Ikai, Chiral HPLC for efficient resolution of enantiomers, Chem. Soc. Rev. 37 (2008) 2593–2608.

[7] T. Ikai, Y. Okamoto, Structure control of polysaccharide derivatives for efficient separation of enantiomers by chromatography, Chem. Rev. 109 (2009) 6077–6101.

[8] J. Shen, T. Ikai, Y. Okamoto, Synthesis and application of immobilized polysaccharide-based chiral stationary phases for enantioseparation by high-performance liquid chromatography, J. Chromatogr. A 1363 (2014) 51–61.

[9] P. Peluso, V. Mamane, E. Aubert, S. Cossu, Insights into the impact of shape and electronic properties on the enantioseparation of polyhalogenated 4,4’-bipyridines

on polysaccharide-type selectors. Evidence for stereoselective halogen bonding interactions, J. Chromatogr. A 1345 (2014) 182–192.

[10] R.B. Kasat, S.Y.Wee, J.X. Loh, N.-H.L.Wang, E.I. Franses, Effect of the solute molecular structure on its enantioresolution on cellulose tris(3,5-dimethylphenylcarbamate), J. Chromatogr. B 875 (2008) 81–92.

[11] A. Del Rio, Exploring enantioselective molecular recognition mechanisms with chemoinformatic techniques, J. Sep. Sci. 32 (2009) 1566–1584.

[12] R. Sheridan, W. Schafer, P. Piras, K. Zawatzky, E.C. Sherer, C. Roussel, C.J. Welch, Toward structure-based predictive tools for the selection of chiral stationary phases for the chromatographic separation of enantiomers, J Chromatogr. A 1467 (2016) 206–213.

[13] T.D. Booth, I.W. Wainer, Mechanistic investigation into the enantioselective separation of mexiletine and related compounds, chromatographed on an amylose tris(3,5-dimethylphenylcarbamate) chiral stationary phase, J. Chromatogr. A 741 (1996) 205–211.

[14] C.A. Montanari, Q.B. Cass, M.E. Tiritan, A.L. Soares de Souza, A QSERR study on enantioselective separation of enantiomeric sulphoxides, Anal. Chim. Acta 419 (2000) 93–100.

[15] L. Pisani, M. Rullo, M. Catto, M. de Candia, A. Carrieri, S. Cellamare, C.D. Altomare, Structure–property relationship study of the HPLC enantioselective retention of neuroprotective 7-[(1-alkylpiperidin-3-yl)methoxy]coumarin derivatives on an amylose-based chiral stationary phase, J. Sep. Sci. (2018) in press.

[16] B. Rasulev, M. Turabekova, M. Gorska, K. Kulig, A. Bielejewska, J. Lipkowski, J. Lleszczynski, Use of quantitative structure–enantioselective retention relationship for the liquid chromatography chiral separation prediction of the series of pyrrolidin-2-one compounds, Chirality 24 (2012) 72–77.

[17] S. Khater, M.A. Lozac'h, I. Adam, E. Francotte, C. West, Comparison of liquid and supercritical fluid chromatography mobile phases for enantioselective separations on polysaccharide stationary phases, J. Chromatogr. A 1467 (2016) 463–472.

[18] M. Szaleniec, A. Dudzik, M. Pawul, B. Kozik, Quantitative structure enantioselective retention relationship for high-performance liquid chromatography chiral separation of 1-phenylethanol derivatives. J. Chromatogr. A 1216 (2009) 6224–6235.

[19] L. Asensi-Bernardi, L. Escuder-Gilabert, Y. Martín-Biosca, M.J. Medina-Hernández, S. Sagrado, Modeling the chiral resolution ability of highly sulfated-β-cyclodextrin for basic compounds in electrokinetic chromatography, J. Chromatogr. A 1308 (2013) 152–160.

[20] L. Escuder-Gilabert, Y. Martín-Biosca, M.J. Medina-Hernández, S. Sagrado, Enantioresolution in electrokinetic chromatography-complete filling technique using sulfated gamma-cyclodextrin. Software-free topological anticipation, J. Chromatogr A 1467 (2016) 391–399.

[21] ChemSpider Database. Royal Society of Chemistry. http://www.chemspider.com/ (accessed 21.2.18).

[22] L. Escuder-Gilabert, J.M. Sanchis-Mallols, S. Sagrado, M.J. Medina-Hernández, R.M. Villanueva-Camañas, Chromatographic quantitation of the hydrophobicity

of ionic compounds by the use of micellar mobile phases, J. Chromatogr. A 823 (1998) 549-559.

[23] C. Hansch, in: Comprehensive Medicinal Chemistry, Vol 6, Pergamon Press, New York, 1st ed., 1990.

[24] CAMO Software AS. http://www.camo.com/ (accessed 21.2.18).

[25] S. Sagrado, M.T.D. Cronin, Diagnostic Tools to Determine the Quality of "Transparent" Regression-Based QSARs: The "Modelling Power" Plot, J. Chem. Inf. Model. 46 (2006) 1523-1532.

Figure captions

Fig. 1. Unscrambler® PCA results. (A) PC1-PC2 bi-plot showing the scores (relationships between compounds; +) and loadings (relationships between variables; ○). (B) Influence plot (Residual vs. Leverage) for the compounds studied.

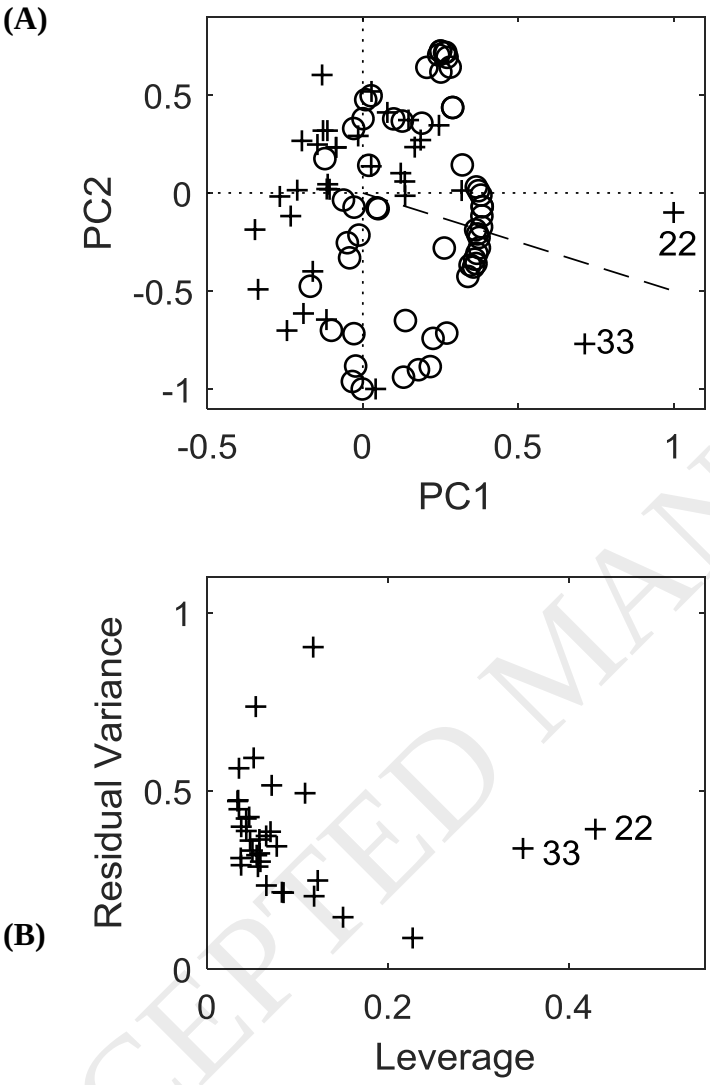

Fig. 1

Fig. 2. DPLS1 outputs as a function of the number of remaining variables in the model during the first stage of the refinement process. Explained (*EV*, ×) and cross-validated (EV_{CV}, +) variance values for the response variable, predictive power (*Pp*, ○) and optimal number of latent variables (k_o, —).

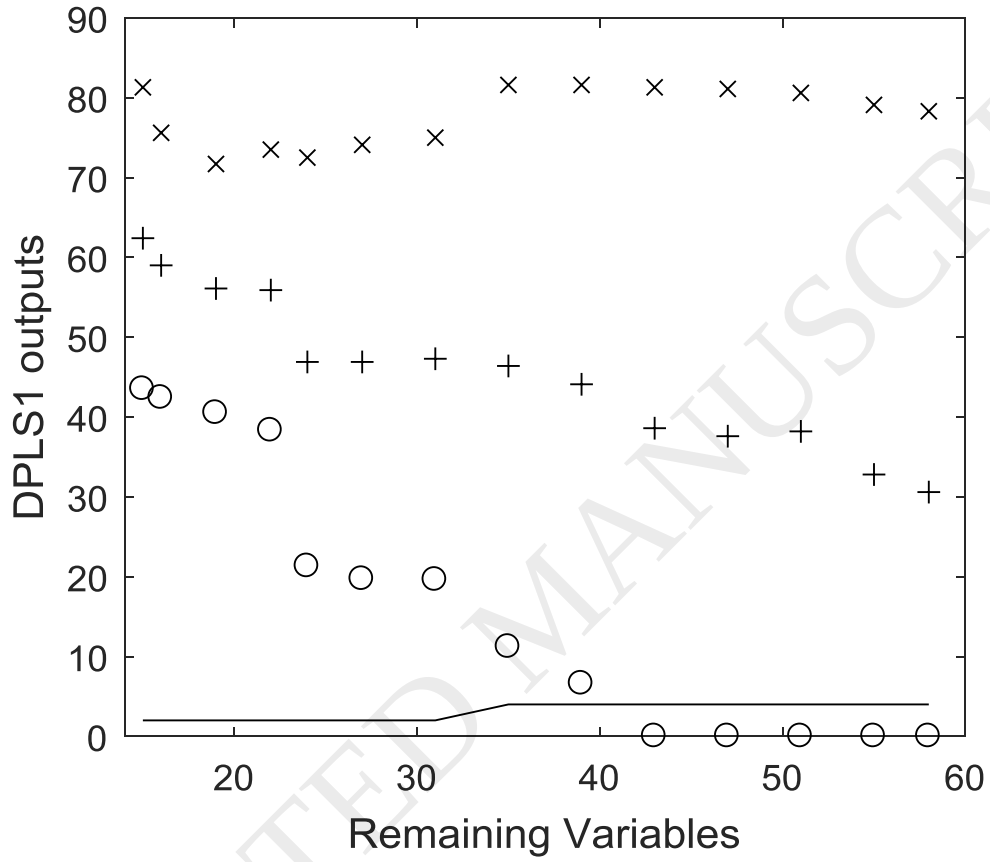

Fig. 2.

Fig. 3. Final (refined) DPLS1 score plot. Compounds are labelled by their (A) numbered order (*No*), (B) categorical enantioresolution (*RsC*) and (C) drug/pesticide family. See further details in Table 1.

(A)

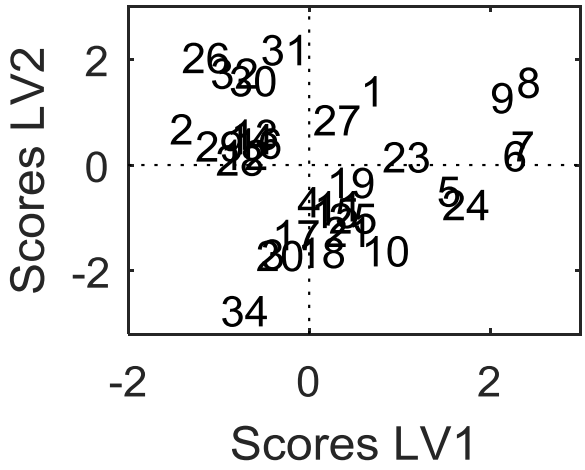

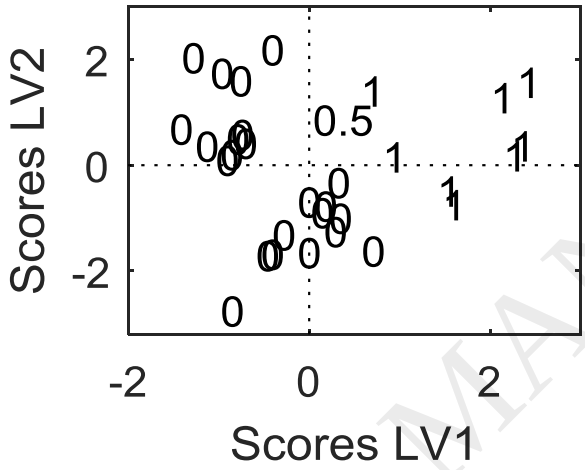

(B)

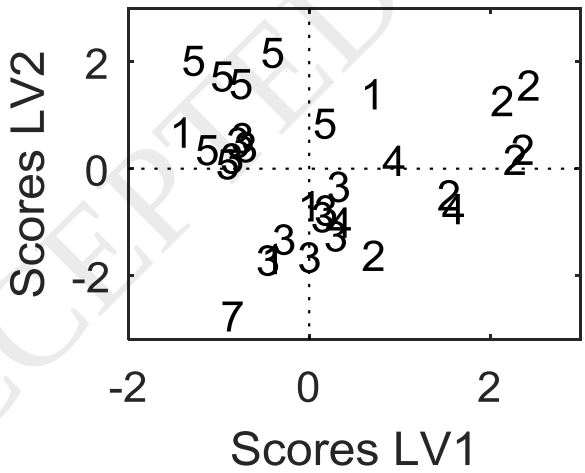

(C)

Fig. 3

Fig. 4. Enantioresolution discriminant ability of eq. 5. Estimates from eq. 5 (*eRs* outputs) *vs*. *RsC* values from Table 1. Horizontal lines at 0.4 and 0.5 separate the three initial *RsC* levels (0, 0.5 and 1).

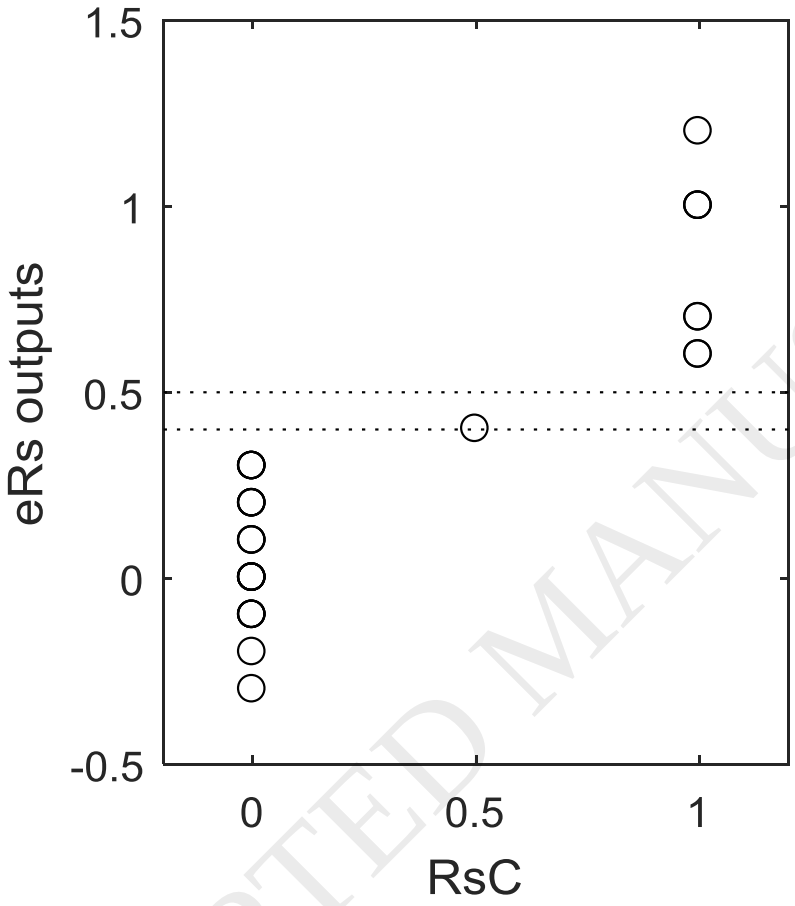

Fig. 4.

Table 1

Experimental enantioresolution data (*Rs*). Compounds are identified by their name and numbered order (*No*). Categorical enantioresolution (*RsC*) levels are assigned according to the experimental observations: *RsC* = 1 if *Rs* > 1.7; otherwise, *RsC* = 0 (with the exception of propranolol; *RsC* = 0.5 since *Rs* = 1.4). Structural influence investigated by principal components analysis (PCA). The 2D molecular structure can be seen in Table S1 (Supplementary data).

Name	*No*	Family [a]	*Rs*	*RsC*	Structural influence [b]
Nomifensine	1	1	6.5	1	
Citalopram	2	1	0.9	0	
Fluoxetine	3	1	0	0	
Viloxazine	4	1	0	0	
Benalaxyl	5	2	6.3	1	
Imazalil	6	2	3.7	1	
Penconazole	7	2	3.6	1	
Hexaconazole	8	2	2.7	1	
Myclobutanil	9	2	1.7	1	
Metalaxyl	10	2	0	0	
Trimeprazine	11	3	0.5	0	
Doxylamine	12	3	1.0	0	
Brompheniramine	13	3	0.6	0	
Chlorpheniramine	14	3	0.5	0	
Orphenadrine	15	3	0.3	0	
Carbinoxamine	16	3	0	0	
Clemastine	17	3	0	0	
Ethopropazine	18	3	0	0	
Hydroxyzine	19	3	0	0	
Methotrimeprazine	20	3	0	0	
Promethazine	21	3	0	0	
Terfenadine	22	3	0	0	Influential
Mepivacaine	23	4	2.2	1	
Propanocaine	24	4	2.2	1	
Prilocaine	25	4	0.7	0	
Pindolol	26	5	0	0	
Propranolol	27	5	1.4	0.5	
Metoprolol	28	5	0.3	0	
Acebutolol	29	5	0	0	
Atenolol	30	5	0	0	
Salbutamol	31	5	0	0	
Timolol	32	5	0	0	
Verapamil	33	6	0.6	0	Influential
Methadone	34	7	1.0	0	

[a] Drug/Pesticide families: 1 (antidepressants), 2 (fungicides), 3 (antihistamines), 4 (local anaesthetics), 5 (β-blockers), 6 and 7 (other families of drugs).

[b] Influential compounds (with dissimilar structure) are not used to build the discriminant model.

Table 2

Variables selected in the final discriminant partial least squares (DPLS1) model: heteroatoms linked to the chiral carbon (*C**X), aromatic heterocycles linked to the chiral carbon (*C**hA), minimal z length (*zmin*), molecular surface area (*MSA*), orbital electronegativity of the chiral carbon atom (*OEC**), surface tension (*ST*), aromatic ring count (*Arc*), apparent logarithm of octanol–water partition coefficient (log*D*) and molar total charge (α). Their contribution sign to the enantioresolution is indicated in brackets. Anticipated-*RsC* values (*aRsC*) after rounding the *eRs* outputs (eq. 5) to integer values.

No	*C*X* (-)	*C*hA* (-)	*zmin* (-)	*MSA* (-)	*OEC** (+)	*ST* (+)	*Arc* (+)	log*D* (+)	α (-)	*aRsC*
1	0	0	7.05	374.70	8.42	46.60	2	1.22	0.88	1
2	1	1	10.86	499.26	9.10	49.90	2	0.72	0.98	0
3	1	0	8.89	449.60	8.83	33.00	2	2.28	0.98	0
4	1	0	7.40	391.60	8.86	36.80	1	0.69	0.61	0
5	1	0	9.68	520.10	8.97	44.50	2	3.88	0.00	1
6	1	0	7.71	382.90	8.92	40.80	2	3.56	0.06	1
7	0	0	7.66	389.70	8.25	42.90	2	3.66	0.00	1
8	0	0	8.17	432.90	9.00	46.10	2	3.66	0.00	1
9	0	0	8.56	423.80	8.92	44.70	2	2.82	0.00	1
10	1	0	9.14	459.43	8.48	40.50	1	2.15	0.00	0
11	0	0	7.69	469.40	7.82	43.50	2	3.54	0.96	0
12	1	1	8.79	463.90	9.23	39.30	2	1.60	0.88	0
13	0	1	9.32	432.60	8.58	43.10	2	2.08	0.97	0
14	0	1	9.29	428.51	8.58	42.10	2	1.91	0.97	0
15	1	0	8.73	467.00	8.99	38.00	2	3.20	0.88	0
16	1	1	9.53	444.30	9.15	43.00	2	1.84	0.88	0
17	1	0	9.62	549.20	9.06	39.70	2	4.13	0.97	0
18	1	0	8.29	500.40	8.17	42.90	2	4.23	0.98	0
19	1	0	7.78	579.98	8.54	47.80	2	1.81	0.40	0
20	0	0	9.86	518.60	7.82	42.80	2	3.50	0.96	0
21	1	0	8.61	439.30	8.16	44.10	2	3.69	0.92	0
23	1	0	6.44	423.60	8.76	44.00	1	1.86	0.33	1
24	1	0	7.76	522.70	8.86	41.10	2	5.30	0.25	1
25	1	0	8.42	387.30	8.72	38.50	1	1.49	0.44	0
26	0	0	6.92	399.50	8.83	47.50	2	-0.57	1.86	0
27	0	0	8.31	426.90	8.83	42.70	2	1.63	0.97	0
28	0	0	6.50	474.70	8.83	37.10	1	0.11	0.98	0
29	0	0	6.86	560.30	8.83	43.20	1	0.37	0.97	0
30	0	0	5.96	440.41	8.83	45.00	1	-1.58	0.98	0

31	0	0	6.38	405.96	8.84	49.20	1	-1.41	0.96	0
32	0	0	7.75	497.99	8.83	52.50	1	-1.09	0.98	0
34	1	0	10.05	540.01	8.31	37.10	2	3.05	0.93	0

Table 3

Application of the protocol to obtain anticipated enantioresolution values (*aRsC*) for new compounds non included to build the model and experimental enantioresolution values (*Rs*). See further details for other variables in Table 2.

Compound	*C*X* (-)	*C*hA* (-)	*zmin* (-)	*MSA* [a] (-)	*OEC** (+)	*ST* (+)	*Arc* (+)	log*D* (+)	*α* (-)	*eRs* [b]	*aRsC*	*Rs*
Fenfluramine	1	0	8.79	359.91	8.05	26.30	1	0.83	0.99	< 0.4	0	0
Amlodipine	0	0	11.71	570.90	8.42	44.40	1	2.71	0.96	< 0.4	0	0.6
Bupivacaine	1	0	8.21	517.09	8.82	41.60	1	3.30	0.50	< 0.4	0	0.8
Bicalutamide	1	0	6.99	527.46	9.44	58.20	2	4.94	0	> 0.5	1	1.7

[a] Step-1b criterion. *MSA* values are in the 350 – 600 Å^2 range (anticipation can be performed).
[b] Step-3 criterion. *eRs* outputs from eq. 5 used for anticipating *aRsC*: baseline enantioresolution (*aRsC* = 1) if *eRs* > 0.5 and poor or non enantioresolution (*aRsC* = 0) if *eRs* < 0.4.